CONTENTS

LIST OF FIGURES

LIST OF TABLES

LISTINGS

ACRONYMS

AGN	Active Galactic Nuclei
NLR	Narrow Line Region
BLR	Broad Line Region
EV1	Eigenvector 1
ICA	Independent Component Analysis
PCA	Principal Component Analysis
SDSS	Sloan Digital Sky Survey
BOSS	Baryon Oscillation Spectroscopic Survey
UV	Ultra-Violet
EQW	Equivalent Qidth
S/N	Signal-to-noise
BH	Black Hole

SED	Spectral Energy Distribution
IR	Infrared
NIR	Near-infrared
FWHM	Full-Width-at-Half-Maximum

1 INTRODUCTION

1.1 DISCOVERY

The first quasar was discovered when it was found that the star-like, thirteenth magnitude objected associated with the radio source 3C 273 was at a cosmological distance ($z = 0.158$; Schmidt, 1963). This implied an enormous luminosity ($4 \times 10^{12} L_{\odot}$) for such a compact object and it was quickly realised that energy source was the release of gravitational potential energy as mass is accreted onto a super-massive black hole (BH) at the centre of a galaxy (e.g. Hoyle and Fowler, 1963; Salpeter, 1964; Lynden-Bell, 1969; Lynden-Bell and Rees, 1971).

Super-massive: $10^{6-9}\ M_{\odot}$

1.2 BASIC STRUCTURE

An Active Galactic Nucleus[1] (AGN) is significantly more compact than a cubic parsec, and yet can outshine the starlight from an entire galaxy. The basic features of the current paradigm explaining this phenomenon are essentially unchanged from Salpeter, (1964), although many of the details remain unclear. Material is pulled towards a super-massive BH and sheds angular momentum through viscous and turbulent processes in a hot accretion disc (e.g. Begelman, 1985). The accretion disc reaches temperatures of $\sim 10^6$K, and radiates primarily at ultraviolet (UV) to soft-X-ray wavelengths. Hard X-ray emission originates in a hot corona near the BH, emission lines are produced in rapidly moving clouds of ionised gas and infrared emission is dominated by thermal emission from a dusty, parsec-scale structure. Collimated jets of relativistic plasma and/or associated lobes are also seen in the 10 per cent of quasars that are radio-loud (e.g. Peterson, 1997).

1.2.1 *The broad line region*

One of the pre-eminent features of many AGN spectra are broad optical and UV emission lines produced in the *broad line region (BLR)*. The BLR consists of gas clouds at distances from several light-days to several light-months that are photo-ionised by the ultraviolet continuum emission emanating from the accretion disc. Because of the

1 Throughout this thesis we use the terms 'quasar' and 'Active Galactic Nucleus (AGN)' interchangeably to describe active supermassive black holes, although the term quasar is generally reserved for the luminous ($L_{Bol} > 10^{12} L_{\odot}$) subset of AGNs.

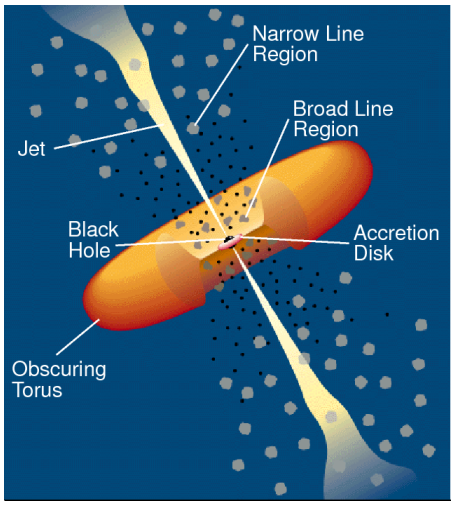

Figure 1.1: Illustration of the physical structure of an AGN in a simple orientation-based unification model. Figure taken from Urry and Padovani, (1995).

close proximity to the central super-massive BH, bulk motions are dominated by gravity and radiation pressure. The very broad emission line widths are assumed to Doppler-broadened, and imply line-of-sight velocities of many thousands of $\mathrm{km\,s^{-1}}$.

1.2.2 *The dusty torus*

Further out are dusty, molecular clouds which are co-planar with the accretion disc. These dusty clouds are generally referred to as the 'torus'. In a Type II AGN, the accretion disc is observed in an edge-on configuration and, as a result, emission from the accretion and BLR is obscured by the dusty torus (e.g. Antonucci, 1993). Although this simple picture (shown in Figure 1.1) is a useful staring point, the idea of a torus as a static, doughnut-like structure is almost certainly incorrect. For example, the problem of maintaining the thickness of such a structure has long been recognized. In one alternative scenario, the torus is the dusty part of an accretion disc wind that extends beyond the dust-sublimation radius (e.g. Konigl and Kartje, 1994; Everett, Gallagher, and Keating, 2009; Gallagher et al., 2012; Everett, 2005; Keating et al., 2012; Elitzur and Shlosman, 2006).

1.2.3 *The narrow line region*

Further away from the central BH and beyond the dusty torus is the narrow emission line region (NLR). Like the BLR, the NLR is ionised by radiation from the central source. Unlike the BLR, densities in the NLR are low enough that forbidden transitions are not collisionally

suppressed. Emission line widths are typically hundreds of $\mathrm{km\,s^{-1}}$ in the NLR. The NLR is sufficiently extended to be spatially resolved.

Extent: ask Paul/Manda

1.3 WINDS AND OUTFLOWS IN AGN

Quasars are very powerful sources of radiation, and are embedded in matter-rich environments at the centres of galaxies. Strong winds, driven by some combination of gas pressure, radiation pressure due to dust or lines, and magnetic forces, are to be expected under these conditions (e.g. Blandford and Payne, 1982; Proga, Stone, and Kallman, 2000; Everett, 2005). In line with these expectations, evidence for outflows is common in the spectra of quasars.

Perhaps the most dramatic evidence of outflows is seen in broad absorption line quasars (BALQSOs; Weymann et al., 1991). BALQSOs are characterised by broad absorption features in the ultra-violet resonance lines of highly ionised N V, C IV and Si IV. The absorption is always blueshifted, and is evidence for fast outflows with velocities as large as $60\,000\ \mathrm{km\,s^{-1}}$ (e.g. Turnshek, 1988). The observed C IV BALQSO fraction in radio-quiet quasars is ~ 15 per cent (e.g. Hewett and Foltz, 2003; Reichard et al., 2003) and the intrinsic fraction has been estimated at 40 per cent (Allen et al., 2011). The blueshifting of high-ionisation lines in the BLR (including C IV) also appears to be nearly ubiquitous in the quasar population (e.g. Richards et al., 2002; Richards et al., 2011), suggesting winds are even more common. Outflows are also used to explain narrow UV and X-ray absorption lines (NALs) which are seen in ~ 60 per cent of Seyfert 1 galaxies (Crenshaw et al., 1999) and some quasars (e.g. Hamann et al., 1997). The wide range of emission and absorption line phenomena can be explained in disc wind models (e.g. Murray et al., 1995; Elvis, 2000; Proga, Stone, and Kallman, 2000; Everett, 2005)

1.4 SDSS AND THE ERA OF SURVEY ASTRONOMY

Emphasise the range of data now available and this allows us to do

1.5 THE AGN-HOST GALAXY CONNECTION

The space density of quasars was much greater at $z \gtrsim 2$, and declines steeply to $z = 0$. The existence of inactive BHs at the centres of massive galaxies is therefore a fundamental test of the quasar paradigm. Significant resources have been devoted to searching for these BHs, which are now known to exist in the centres of many nearby massive galaxies (e.g. Kormendy and Richstone, 1995; Ferrarese and Ford, 2005; Kormendy and Ho, 2013). Remarkably, given the sphere-of-influence of the BH is many orders of magnitude smaller than the size of the galaxy, the BH mass and mass of the host galaxy spheroid

are strongly correlated (Ferrarese and Merritt, 2000; Gebhardt et al., 2000; Graham et al., 2001; Tremaine et al., 2002; Marconi and Hunt, 2003; Aller and Richstone, 2007; Gültekin et al., 2009). Although any underlying causal mechanism(s) responsible for the correlation is yet to be conclusively identified, there is considerable observational and theoretical support for a 'feedback' relationship in which the energy output from rapidly accreting BHs (in a quasar phase) couples with the gas in the host galaxy and quenches star formation (e.g. Silk and Rees, 1998; King, 2003; Di Matteo, Springel, and Hernquist, 2005; King and Pounds, 2015).

Models of galaxy evolution that invoke AGN feedback require these outflows to reach galactic scales and quench star formation in the AGN host galaxies. In recent years, a huge amount of resources have been devoted to searching for observational evidence of these galaxy-wide, AGN-driven outflows. This has resulted in recent detections of outflows in AGN-host galaxies using tracers of atomic, molecular, and ionised gas with enough power to sweep their host galaxies clear of gas (e.g. Nesvadba et al., 2006; Arav et al., 2008; Nesvadba et al., 2008; Moe et al., 2009; Dunn et al., 2010; Alexander et al., 2010; Harrison et al., 2012; Harrison et al., 2014; Nesvadba et al., 2010; Rupke and Veilleux, 2013; Veilleux et al., 2013; Nardini et al., 2015; Feruglio et al., 2010; Alatalo et al., 2011; Cimatti et al., 2013; Cicone et al., 2014).

Quasar feedback has also been invoked to explain the similarity of the cosmic BH accretion and star formation histories. The number density of quasars, which evolves strongly with redshift, peaks at redshifts $2 \lesssim z \lesssim 3$ (e.g. Brandt and Hasinger, 2005; Richards et al., 2006) and the most massive ($M_\bullet \gtrsim 10^9 M_\odot$) present-day BHs experienced much of their growth during this epoch. The star formation rate, which closely follows the cosmological evolution of the quasar luminosity function, also peaks during this epoch (e.g. Boyle and Terlevich, 1998). Quantifying the growth-rate of massive BHs at $2 \lesssim z \lesssim 3$ would therefore help significantly in understanding the role quasars play in galaxy evolution.

1.6 MEASURING BLACK HOLE MASSES

As one of just two fundamental quantities describing a BH on astrophysical scales, the mass is of crucial importance to virtually all areas of quasar science, including the evolution and phenomenology of quasars, and accretion physics. The power output of quasars is directly proportional to the BH mass. There is much debate regarding what effect the energy output by quasars has on the evolution and structure of the host galaxy.

The masses of BHs in many local, inactive galaxies have been measured by dynamical modelling spatially resolved kinematics. How-

ever, this requires the sphere-of-influence of the BH, R_{BH} , to be resolved. With BH masses only ~0.1 per cent of the stellar mass of the host galaxies, $R_{BH} \sim 1 - 100$ pc. With current instrumentation, resolving this region is only possible in very close by galaxies.

$R_{BH} = \frac{2GM_{BH}}{\sigma*}$

The reverberation mapping method, first proposed by Blandford and McKee, (1982), uses the time delay between continuum variations and emission-line variations to estimate the size of the BLR, and hence the BH mass. Because it depends on temporal resolution rather than spatial resolution, this technique can be applied out to much greater distances.

1.6.1 *Reverberation mapping*

Continuum variability is a common characteristic of quasars, owing to the stochastic nature of the accretion process. Because the BLR is photo-ionized by the continuum, the broad emission lines also vary with some characteristic lag, which is related to the light travel time across the BLR. The reverberation mapping technique uses the time lag between variations in the continuum emission and correlated variations in the broad line emission to measure the typical size of the BLR (e.g. Peterson, 1993; Netzer and Peterson, 1997; Peterson, 2014).

Under the assumptions that the BLR dynamics are virialised and the gravitational potential is dominated by the BH, the BH mass is given by:

The virial theorem states...

$$M_{BH} = f\left(\frac{\Delta V^2 R}{G}\right) \tag{1.1}$$

where ΔV is the line-width and R is the reverberation BLR radius. In practice, reverberation mapping relies on dense spectrophotometric monitoring campaigns which span many years. The typical velocity in the BLR is measured from the width of the broad Hβ line. Since the structure and geometry of the BLR is unknown, a virial coefficient f is introduced to transform the observed line-of-sight velocity inferred from the line width in to a virial velocity. In practice, the value of f is empirically determined by requiring that the derived masses are consistent with those predicted from the M-σ relation for local inactive galaxies. Although the reverberation mapping technique has proved to be effective, because it relies on resource-intensive spectrophotometric monitoring campaigns, lags have been measured for only ~ 50 AGN (e.g. Kaspi et al., 2000; Peterson et al., 2004; Kaspi et al., 2007; Bentz et al., 2009; Denney et al., 2010; Barth et al., 2011; Grier et al., 2012). This sample is strongly biased to low luminosity Seyfert 1 galaxies , and the maximum redshift is just $z \sim 0.3$.

σ: velocity dispersion of galaxy

Seyfert 1:

The full width at half maximum (FWHM) or dispersion (σ; derived from the second moment) velocity of the prominent broad emis-

sion line of Hβ (4862.7Å)[2] is used as an indicator of the virial velocity, with extensions to other low-ionization emission lines such as Hα (6564.6Å) and Mg II λλ2796.4,2803.5 (e.g. Vestergaard, 2002; McLure and Jarvis, 2002; Wu et al., 2004; Kollmeier et al., 2006; Onken and Kollmeier, 2008; Wang et al., 2009; Rafiee and Hall, 2011).

FWHM: Full width of the line profile at half of maximum intensity

1.6.2 *Single-epoch virial estimates*

Reverberation mapping campaigns have also revealed a tight relationship between the radius of the BLR and the quasar optical (or ultraviolet) luminosity (the $R-L$ relation; e.g. Kaspi et al., 2000; Kaspi et al., 2007). A slope of $\simeq 0.5$ is found, which consistent with the naive prediction (e.g. Peterson, 1997). An advantage of the technique is that it is inexpensive in telescope time. A single spectrum yields a mass measurement. This relation provides a much less expensive method of measuring the BLR radius, and large-scale studies of AGN and quasar demographics have thus become possible through the calibration of single-epoch virial-mass estimators using the reverberation-derived BH masses (e.g. Greene and Ho, 2005; Vestergaard and Peterson, 2006; Vestergaard and Osmer, 2009; Shen et al., 2011; Shen and Liu, 2012; Trakhtenbrot and Netzer, 2012). Single-epoch virial BH mass estimates normally take the form

$$M_{BH} = 10^{a}\left(\frac{\Delta V}{1000\ \mathrm{km\ s^{-1}}}\right)^{b}\left[\frac{L_{\lambda}}{10^{44}\ \mathrm{erg\ s^{-1}}}\right]^{c} \tag{1.2}$$

where ΔV is a measure of the line width (from either the FWHM or dispersion), L_{λ} is the monochromatic continuum luminosity at wavelength λ, and a, b, and c are coefficients, determined via calibration against a sample of AGN with reverberation-mapping BH mass estimates. Several calibrations have been derived using different lines (e.g. Hβ, Mg II, C IV) and different measures of the line width (FWHM or dispersion) (e.g. Vestergaard, 2002; McLure and Jarvis, 2002; Vestergaard and Peterson, 2006; McGill et al., 2008; Wang et al., 2009; Rafiee and Hall, 2011; Park et al., 2013).

The uncertainties in reverberation mapped BH masses are estimated to be ~ 0.4 dex (e.g. Peterson, 2010), and the uncertainties in virial masses are similar (e.g. Vestergaard and Peterson, 2006). Since the structure and geometry of the BLR is unknown, a virial coefficient f is introduced to transform the observed line-of-sight velocity inferred from the line width in to a virial velocity. This simplification accounts for a significant part of the uncertainty in virial BH masses (in addition to, for example, describing the BLR with a single radius R and scatter in the $R-L$ relation; Shen, 2013). By far the biggest uncertainty is the virial coefficient f . It is unknown, and it probably varies

2 Vacuum wavelengths are employed throughout the thesis.

from source to source. A spherical distribution of clouds on random, isotropic orbits has f = 3/4 for ΔV = FWHM and f = 3 for $\Delta V = \sigma$ (Netzer 1990). Furthermore, if the BLR is anisotropic (for example, in a flattened disk; e.g. Jarvis and McLure, 2006) then the line width will be orientation-dependent (e.g. Runnoe et al., 2013; Shen and Ho, 2014; Brotherton et al., 2015).

The main progress in this area in recent years, that enables comprehensive statistical studies of active black holes (BHs), is the success of the large reverberation mapping project. This allows reliable estimates of broad line region (BLR) sizes and BH masses. The main concern and the biggest unknown is the extension of the method to high redshifts where Hβ measurements are no longer available. Something we will explore in Chapter **??**.

For example, single epoch estimates have been used to calculate black hole masses in the highest redshift quasars to study the growth of SMBHs. This figure shows a compilation of SE mass estimates for quasars over a wide redshift range from different studies. These studies show that massive, 10^9 BHs are probably already in place by $z \sim 7$, when the age of the Universe is less than 1 Gyr. The fact that a SMBH exists in a quasar at such high redshift is of great importance in physics. The high redshift means that it was already there when our universe was very young, only about 800 million years old. And the fact that a SMBH was able to grow up in such a short time put some very tight constraints upon both the cosmological parameters and the accretion history of the SMBH itself (Willott et al. 2003).

Single epoch masses have also been used to study the distribution of quasars in the BH mass-luminosity plane, which conveys important information about the accretion process of these active black holes (e.g. Kollmeier et al. 2016). Redshift evolution of BH-bulge scaling relations (e.g. Bennert et al. 2011). Clustering (Shen & Ho 2014; Timins et al.?). With the R–L relationship, we are able to explore the black hole mass function, not only locally but at high redshift, enabling us to trace the history of black hole growth. Some exploratory work has been done on this and in fact there are claims that the M-sigma relation evolves over time. Estimates of such masses are important with respect to the relation between the MBH in the center of a stellar spheroid and the velocity dispersion.

We emphasize that application of single-epoch spectroscopy to quasars rests on the untested assumption that machinery which is calibrated for sub-Eddington BHs with M$\sim 10^7$ still works for BHs with masses up to 10^{10} that radiate near the Eddington limit. Refer forward to problems with C IV (Chapter 3)

1.7 SEDS

AGN emit strongly over many decades in frequency. To first order SEDs are remarkably similar over many decades in luminosity and redshift. Significant diversity is observed in the SEDs of individual objects. However, the systematic study of the dependence of the SED shape on physical parameters has, until very recently, been limited by the difficulty in obtaining a large sample of quasars with good multi-wavelength coverage and large dynamic range in luminosity and redshift. However, we are able to take advantage of a number of recent, sensitive, wide-field photometric surveys, including SDSS (in the UV/optical), UKIDSS (in the NIR) and WISE (in the mid-infrared).

1.8 SUMMARY / WHAT I NEED TO GET ACROSS

It's a data rich time. SDSS has been revolutionary - shown the power of large surveys. We have wide-field photometry in a number of bands - important because AGN emit strongly over many decades in frequency. With spectra from SDSS we can derive BH masses and outflow properties from optical lines. But these are shifted to infrared wavelengths at redshifts > 1, when things get interesting. Increasing availability of infrared-spectra. Looking to the future, huge spectroscopic surveys - WEAVE, 4MOST.

Quasar black hole masses: Shen, (2013), Peterson, (2010), Peterson, (2011), Vestergaard et al., (2011), Marziani and Sulentic, (2012). This has motivated a considerable amount of observational work searching for feedback signatures (for recent reviews, see Alexander and Hickox, 2012; Fabian, 2012; Heckman and Best, 2014).

Throughout this thesis we adopt a ΛCDM cosmology with $h_0 = 0.71$, $\Omega_M = 0.27$, and $\Omega_\Lambda = 0.73$. All wavelengths and equivalent width measurements are given in the quasar rest-frame, and all emission line wavelengths are given as measured in vacuum.

Get across:

Quasars are not all the same! There is a large range of continuum, emission, and absorption properties among quasars, which demands that quasars cannot be fully described by a single, static picture.